Original Article

Investigation of Thermal and Electrical Conductivity of Chemically Synthesized Poly[(ortho-toldine-co-(2-hydroxy-4-methyl anline)] Composite Doped with HCl

Samia Mezhr Merdas, Samah Hussein Kadhim*

Department of Chemistry, College of Science, University of Thi-Qar, Iraq

ABSTRACT

New electrically conducting composite polymers consisting of poly (2-hydroxy-5-methyl anline) self-doped with poly (*o*-toluidine) were prepared within the polymer matrix by in situ polymerization of aniline. The conversion yield of self-doped poly[2-hydroxy-5-methyl anline-co-(*o*-toluidine)] into doped poly[2-hydroxy-5-methyl anline-co-(o-toluidine)] by treatment with HCl while structural confirmation of the synthesized polymer was sought by Fourier Transform Infrared and thermogravimetric analysis. Conductivity of the polymers was measured by two probe method. As for Activation energy, Ea for dc conduction was deduced and its value was found to be the fraction of an eV for all the polymers. By increasing doping content, Ea decreased and σ increased. The result showed that the conductivity increased with increasing temperature in the order: Doping P(OT-co-HMA)> P(OT-co-HMA)> PHMA >POT, showing conducting behavior and activation energy of polymers was estimated.

GRAPHICAL ABSTRACT
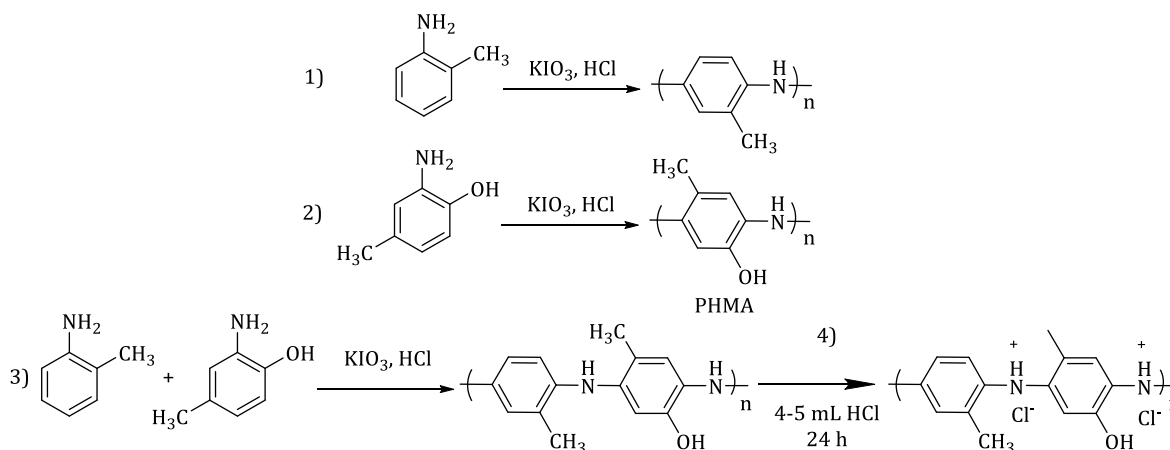
* Corresponding author: Samah Hussein Kadhim
✉ E-mail: Email: Samah.h_chem_chem@sci.utq.edu.iq

Introduction

Conductive polymers can be considered as advanced polymers to be utilized in variation of industries. Intrinsically conductive polymers (ICPs) were discovered in 1960. Conducting polymers opened the path to progress in conception the essential chemistry and physics of π-bonded macromolecules. Chemical or electrochemical polymerizations are widely used for the synthesis of conducting polymers from a monomer solution containing an electrolyte salt. The conductive properties of CPs give these polymers an importance to be the raw materials of a wide range of applications inclusive electronic industry [1,2], energy storage [3-6] and photovoltaic devices [7], electrochromic displays [8,9], electrocatalysis, sensors and photocatalysis [10-18]. CPs has drawn increasing attention in biomedicine because they can convert different types of signals into electrical signals. Since the 1980s, when it was found that these materials are compatible with many biological molecules, their biomedical applications have expanded greatly [19]. Due to their excellent biocompatibility, these "smart materials" may be used in different areas of biomedicine [20,21], such as cell (cell growth and cell migration) and tissue engineering, biosensors, drug and gene delivery system, artificial muscles and diagnostic applications [22].

Materials and Methods

o-Toluidine, 2-hydroxy-5-methyl anline, HCl and KIO$_3$ were obtained from sigma Aldrich and the purity 99%.

Instruments

Thermal analysis was carried out using thermal gravimetry analysis (TGA) (Perkin Elmer-TGA-4000) in college of science, university of Muthanna. At the heating rate 2°C /min in range of temperature 40-605 under nitrogen atmosphere with flow rate of 20ml/min., the Fourier transform infrared, (FT-IR) spectra of the samples were recorded (Shimadzu, Japan) in the department of chemistry college of science university of Thi-Qar by KBr disks, at ambient temperature.

Preparation of polymers

Synthesis of poly (o-toluidine)

The initiation of polymerization process of the investigated monomer (o-toluidine) was performed by the drop-wise addition of the oxidizing factor (Potassium Iodate). This agent was added to an acidified solution. The latter was prepared by the utility of doubly distilled water with fixed stirring at 0-4 °C. The ratio between monomer and oxidizing factor was kept at 1: 1. When the increment was completed, the reaction mixture was remained down continuous stirring for 24 hours. The formed and precipitated polymer was filtered. After the filtration, the product was washed with distilled water until the removal of color and product became colorless. Lastly, the prepared polymer was dried at 70 °C for 12 hours, and this was performed using an oven [23-26] (as represented in Scheme1).

Synthesis of poly (2-hydroxy-5-methyl anline)

Poly (2-hydroxy-5-methyl anline) was synthesized with 1 g of 2-hydroxy-5-methyl anline, which was dissolved in 50 mL, aqueous HCl and 50 mL KIO3 solution. The process achieved accordingly to the study of [23-26] (as shown in Scheme1).

Synthesis of self-doped poly [2-hydroxy-5-methyl anline -co-(o-toluidine)]

Poly[2-hydroxy-5-methyl anline-co-(o-toluidine)] was synthesized by the dissolution of (1:1) 2-hydroxy-5-methyl aniline and o-toluidine in 50 mL aqueous HCl solution separated, followed by 50 mL KIO$_3$ solution and the mentioned. The self-doped term was qualified with a method including polymerization in the existence of an acid (with HCl), that is, the polymer that was obtained in the existence of an acid in the system during polymerization was partially doped. Thus, the pre-doping method was done automatically. The second doping process was externally doped [23-26].

Synthesis of doped poly[2-hydroxy-5-methyl anline -co-(o-toluidine)]

A sample of 1 g of synthesized polymer was powdered and then converted in a round-bottomed flask. Hydrochloric acid (HCl) 4-5 mL was diluted in 100 mL of distilled water. The acidic solution was added to the polymer. The new reaction mixt was slowly stirred overnight for 24

hr. at room temperature. Finally, the product was filtered and dried in an oven at 70 °C for 4 hours [23-26] (as shown in Scheme1).
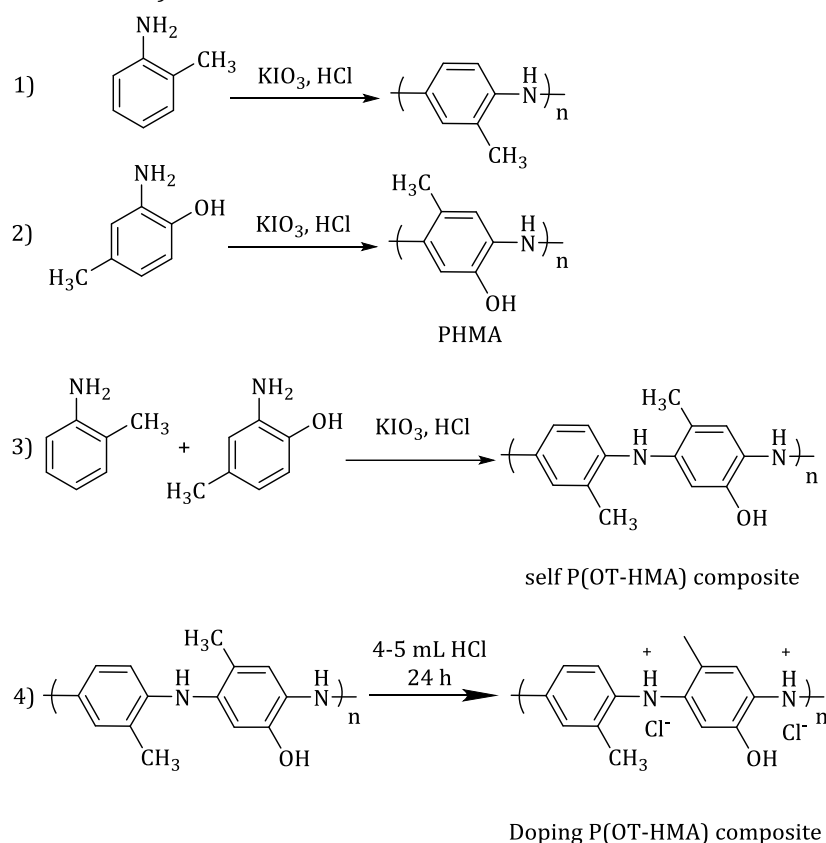
Scheme 1: Preparation of the polymers

Results and Discussion

FT-IR characterization

The FT–IR spectra of POT, PHMA, P(OT-co- HMA) composite and doping P(OT-HA) composite are shown in Figures 1-4. The FT–IR spectrum of POT (Figure 1) displays bands at the rise wavenumber region identical to the N–H stretching mode (3250–3400 cm^{-1}) and the aromatic C–H stretching vibration mode (2850–3000 cm^{-1}). Also, a band located at 1653 cm^{-1} related to the NH$_2$ bending vibration. The adsorption around 1597 and 1483 cm^{-1} are attributed to C=C vibrations of quinonoid and benzenoid rings individually and the intensity of the –CH$_3$ stretching was observed at 2918 cm^{-1}. The peak spotted at 800–900 cm^{-1} is due to a 1,2,4-substitution pattern indicating that the monomeric unit is linked to para location of the ring and a head-to-tail coupling of o-toluidine occurs in polymerization. FT– IR spectrum of PHMA (Figure 2) exhibits a broad band in the 3450-3400 cm^{-1} ranger corresponding for NH stretching and OH stretching. The band around to1606 cm^{-1} is attributed to the NH$_2$ bending vibration. A band, in the 1590-1550 cm^{-1} , 1500-1450 cm^{-1} and 1150-110 cm^{-1} ranger are the characteristic band of quinoid (N=Q=N), benzenoid (N-B-N) and charge position bands, which were observed. The relative intensity of 1600–1500 cm^{-1} is between those of P (OT-co-HMA) composite and doping P(OT-HA) composite (Figure 3-4), so the coexistence of POT and PHMA units in the copolymer was further confirmed (Figure 3-4) [27-28].
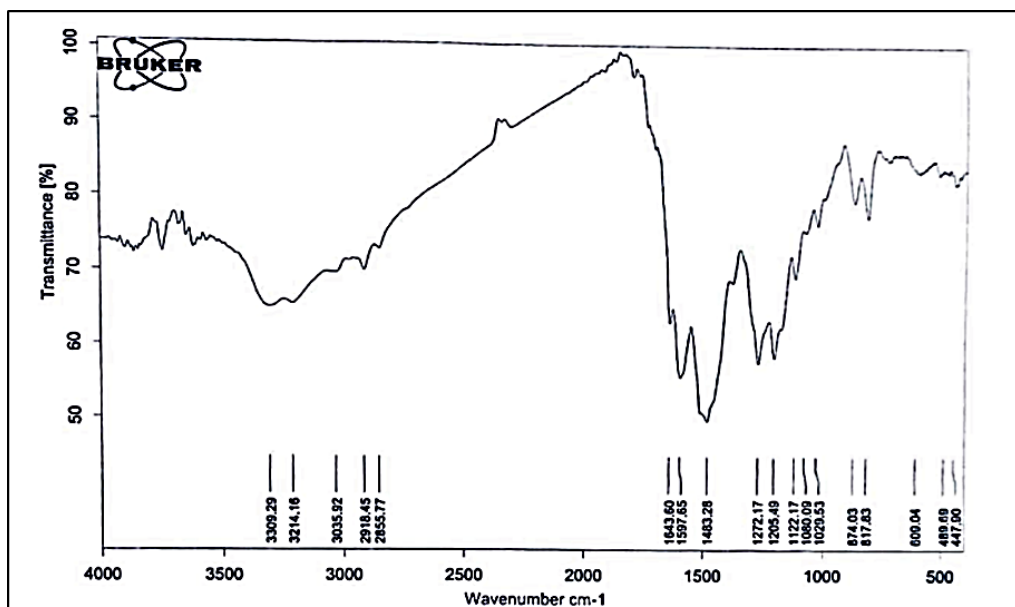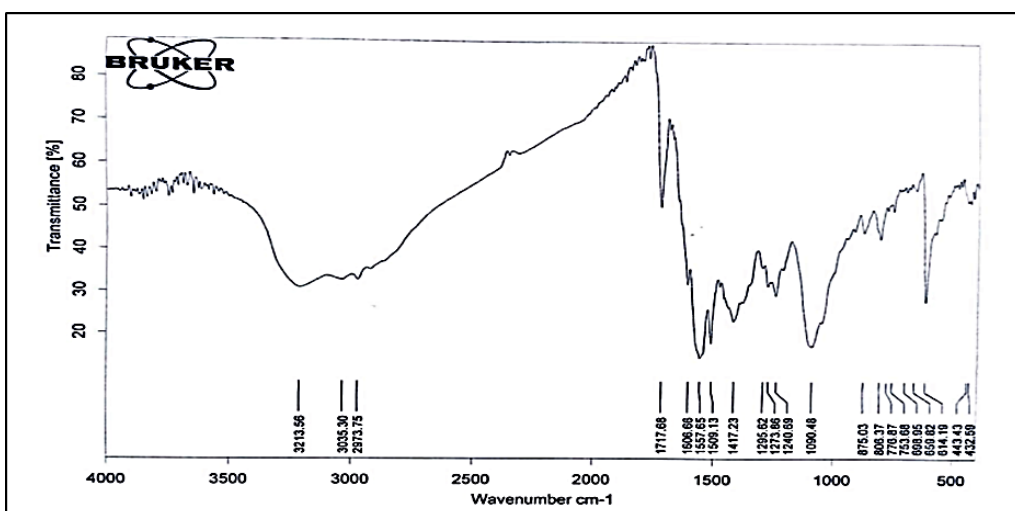
Figure 1: FT–IR spectra of POT
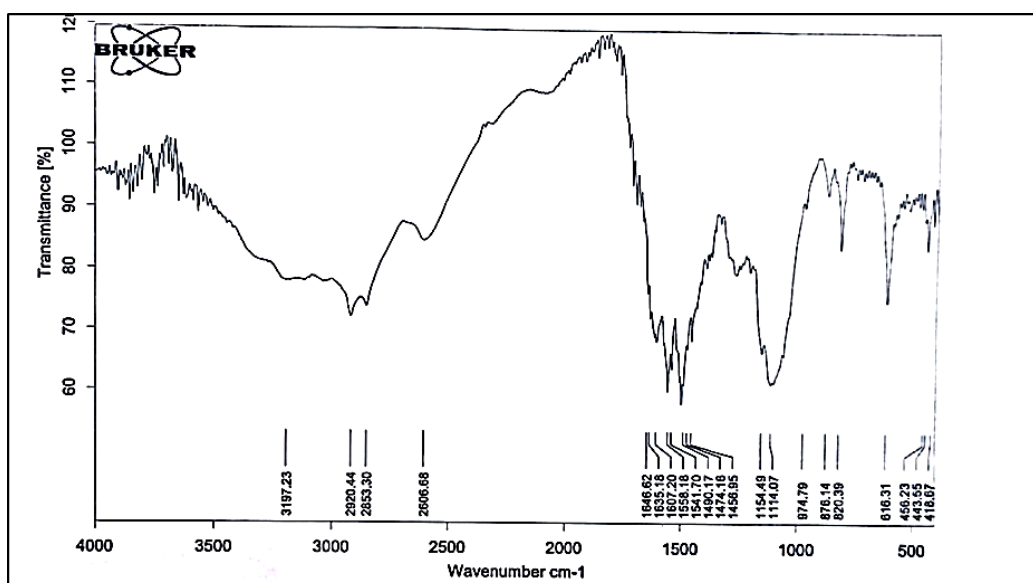

Figure 2: FT–IR spectra of PHMA

Figure 3: FT–IR spectra of P (OT-co- HMA) composite
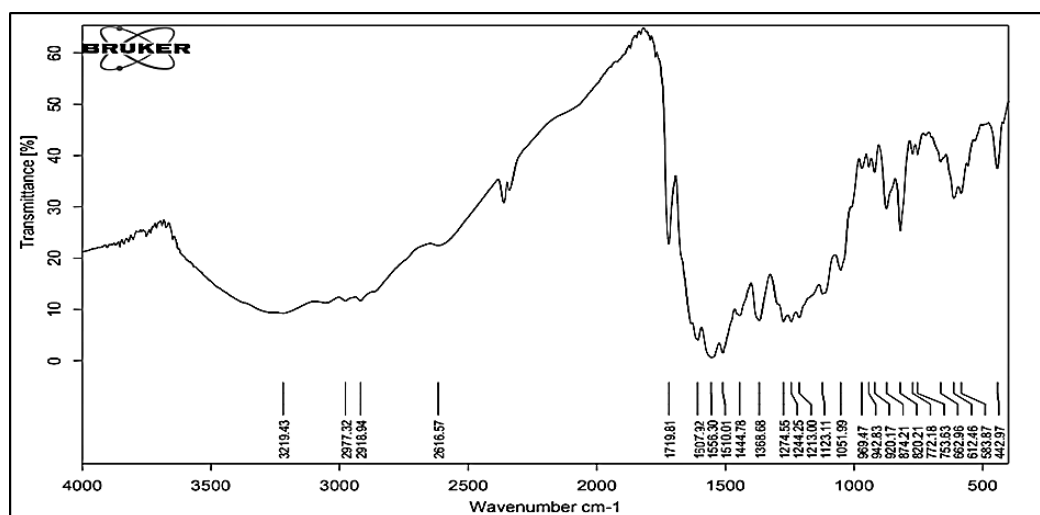
Figure 4: FT–IR spectra of P(OT-HA) composite

Thermogravimetric analysis

The thermal stability of P(OT-co-HMA), POT and PHMA was evaluated by thermogravimetric analysis (TGA) and differential thermogravimetric (DTG). The TGA and DTG curves of P(OT-HMA) composite exhibit higher thermal stability from PHMA and POT curves as shown in Figures 5-8. The TGA curve of PHMA below 150 °C was related to the removal of moisture and low molecular weight polymeric particles; the second stage of mass loss at temperature below 239°C was associated with the decomposition of the polymeric components into volatile water, carbon dioxide and char, while the third stage of mass loss at temperature below 498°C was related to complete degradation of polymer.

The TGA and DTG curves of POT show that there are two stages of mass loss. The first stage weight loss started practically below 170 ˚C. This loss corresponded to the water molecules/ wet from the mold of the polymer. The second one is from 430-738°C, which is associated with the complete decomposition and the polymer backbone.

The tests of TGA and DTG curves of self-doping P(OT-HMA) composite show two stages of mass loss. The first stage weight loss started practically below 187°C corresponding to the water loss molecules/wet available in the polymer mold and low molecular weight polymeric particles. The second stage loss (372-800) °C is associated with the completion of degradation and decomposition of the polymer backbone.

The TGA and DTG curves of doping P(OT-HA) composite exhibit two stages of weight losses. The first stage weight loss occurring within (40-289) ºC is due to the moisture release and release of dopant HCl. The second stage weight loss is due to the structural decomposition of polymer.
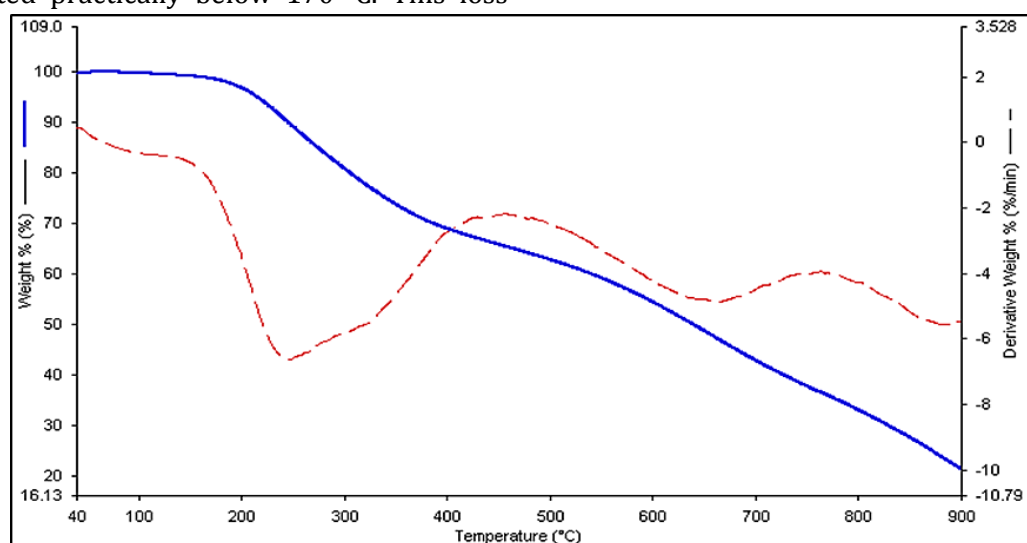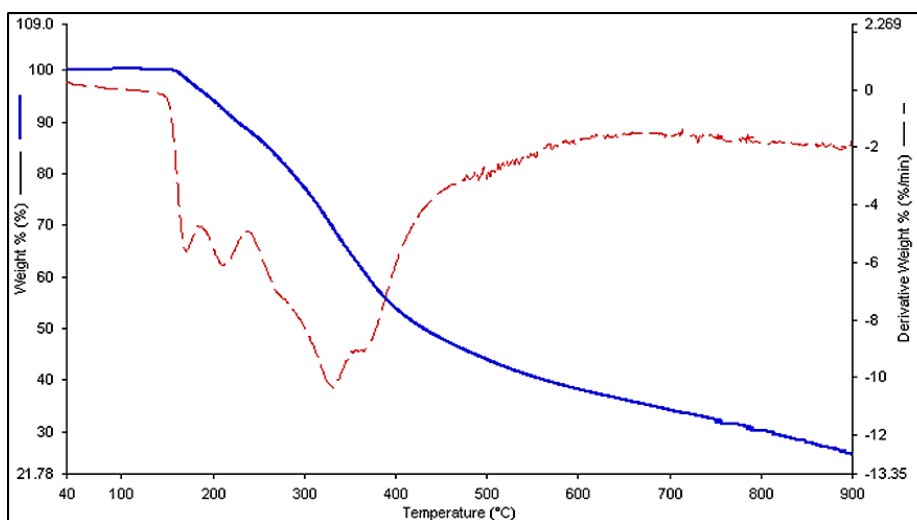

Figure 5: TGA and DTG curves of POT

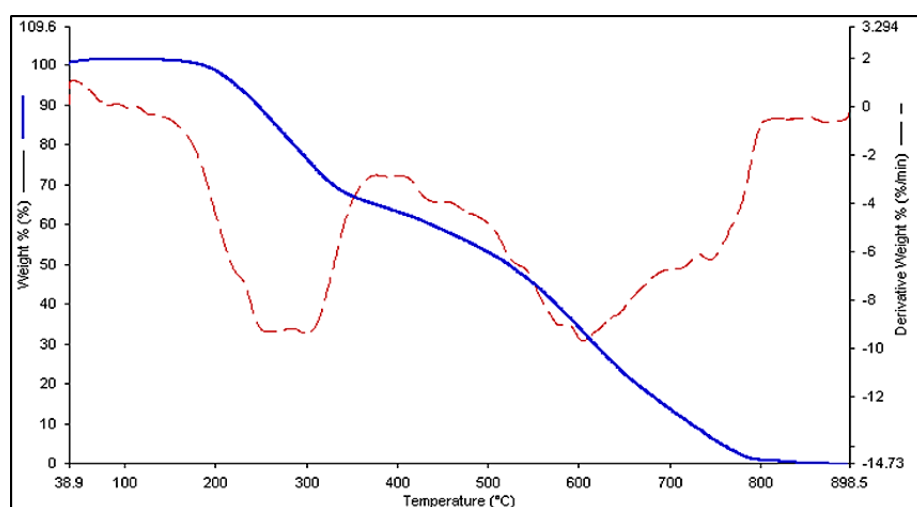**Figure 6:** TGA and DTG curves of PHMA

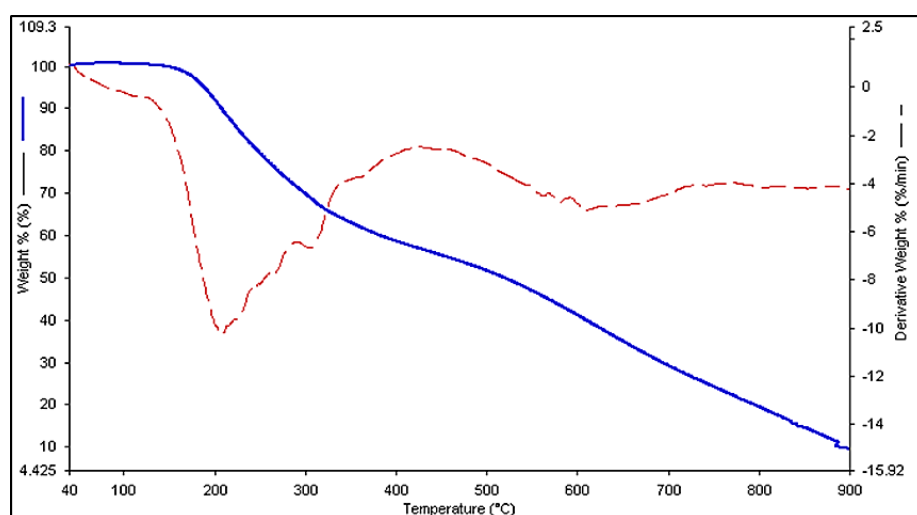**Figure 7:** TGA and DTG curves of P(OT-co-HMA) composite

Figure 8: TGA and DTG curves of doping P(OT-co-HMA) composite

Electrical conductivity

Electrical conductivity σ of the solid material of the POT, PHMA, P(OT-co-HMA) and doping P(OT-co-HMA) in tablets form was measured with a range of temperature of 298-348 K. Measurements of both electrical conductivity and activation energy are listed in Table 1. The following equation describes the relationship of the electrical conductivity with the temperature increase [29]:

$$\sigma = \sigma_o \exp(-Ea/kT) \qquad (1)$$

Where Ea denotes activations energy, and σ_o signifies constant value.

Figures 9-12 illustrate the relationships of the temperature with the range of 293-348 °C with the current voltage characteristics of polymers films. Ohmic behavior was observed at low voltage of less than 3V at, all polymers. The observed increase in the temperature and the applied voltage resemble the properties of semiconductors materials [30].

Higher increase in temperatures led to a new localizing electron with the energy to cross and fill the gap; consequently, the system becomes more ordered. Next, the reduction in the amounting of localized states present will allow for more mobility of charger carriers [31]. Nevertheless, the molecular structure of the polymers hugely affects the charger carriers' mobility, according into the (I-V) characteristics. The electrical conductivity of polymers rises in the order of doping P(OT-co-HMA)> P(OT-co-HMA)> PHMA >POT.

Figures 13-16 show the relationship between ln σ and 1/KT (eV) (Equation 1). The activations of the energy of ligand with complexes can be computed from the slope of the straighter line of the figure. It can be concluded that the value of activations energy declines with the increase of in the order of doping P(OT-co-HMA)> P(OT-co-HMA)> PHMA >POT.

Table1: The electrical conductivities (S/cm) and activations energy (Ea) values for the thin polymers' films

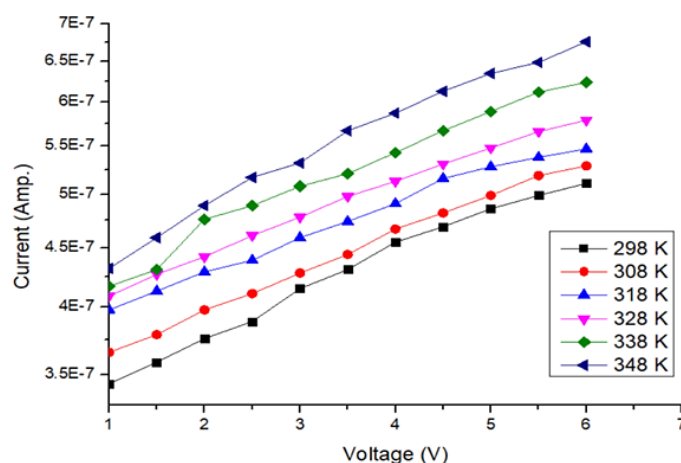| NO	polymers	Electrical conductivity (**S/cm**)	Activation energy (eV)
1	POT	2.1×10^{-8}	0.39
2	PHMA	3.7×10^{-8}	0.30
3	P(OT-co-HMA)	6.9×10^{-5}	0.25
4	doping P(OT-co-HMA)	1.9×10^{-4}	0.20

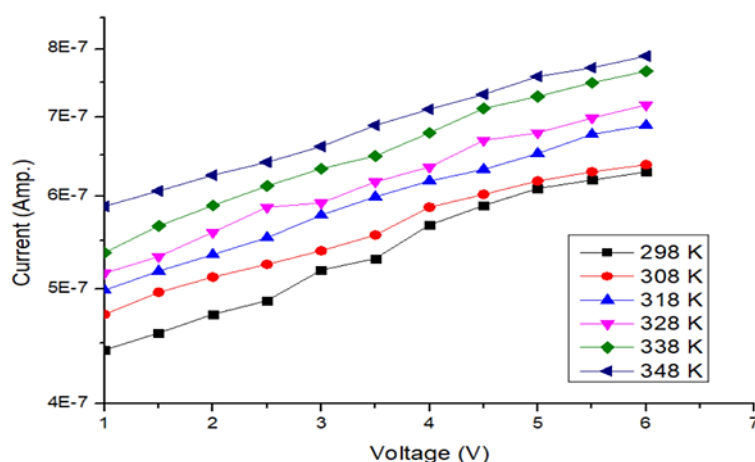**Figure 9:** (I-V) Characteristics at different temperatures for POT

Figure 10: (I-V) Characteristics at different temperatures for PHMA
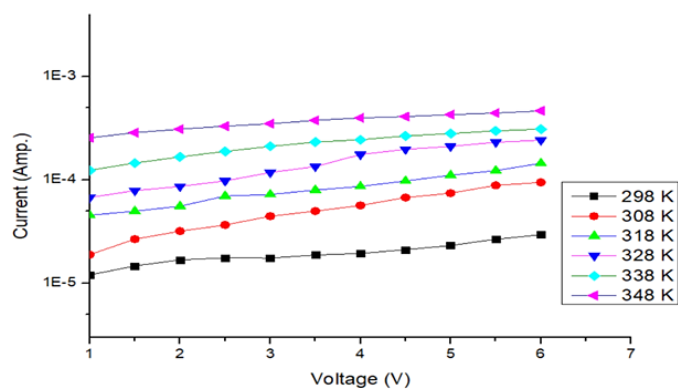
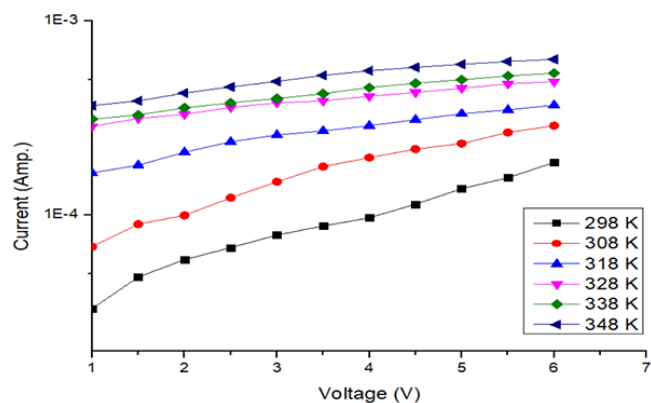**Figure 11:** (I-V) Characteristics at different temperatures for P(OT-co-HMA)

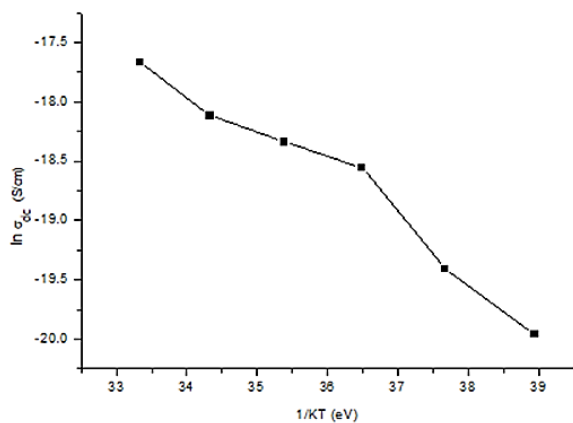**Figure 12:** (I-V) Characteristic at different temperatures for doping P(OT-co-HMA)

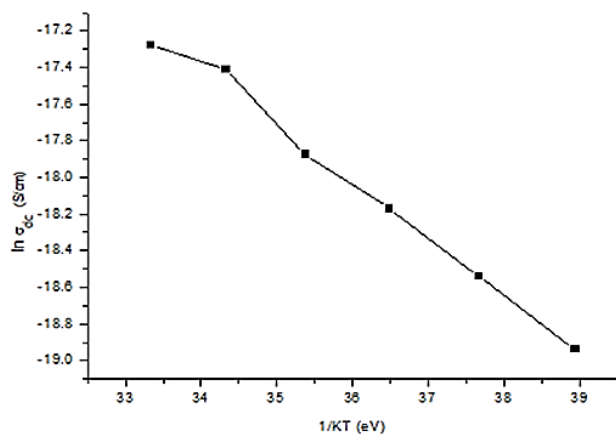**Figure 13:** The relationship between $\ln\sigma_{dc}$ and 1/kT for POT

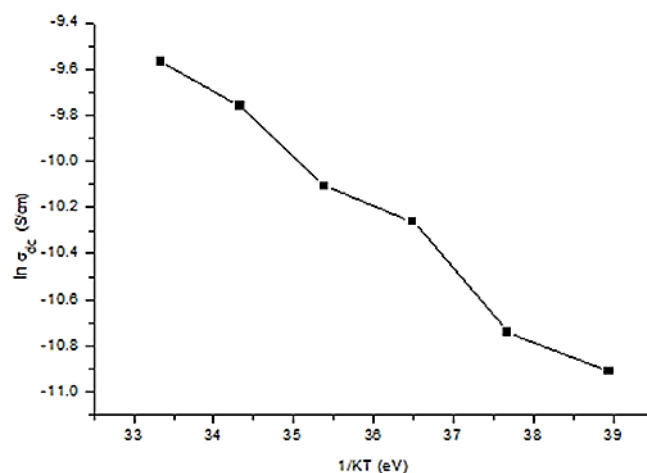**Figure 14:** The relationship between $\ln\sigma_{dc}$ and 1/kT for PHMA

Figure 15: The relationships between $\ln\sigma_{dc}$, and $1/kT$ for P(OT-co-HMA)
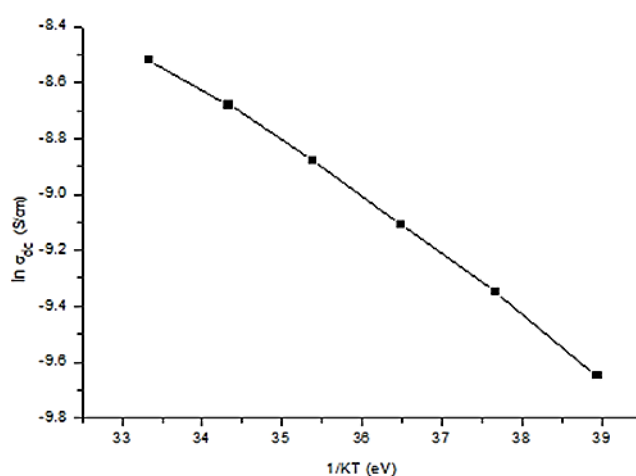

Figure 16: The relationship between $\ln\sigma_{dc}$ and $1/kT$ for doping P(OT-co-HMA)

Figures 17 and 18 show the relations between influence of temperatures and dc conductivity for POT, PHMA, P (OT-co-HMA) and doping P (OT-co-HMA), respectively. The σ_{dc} rises with temperature decline from 25-75 °C, which was due to rising charges carrier in conduction band. This is an indicator of semiconductor-such as manner, which is fit suitable to the following Arrhenius exponential equation (1). The significant excess of dc conductivity between 330 K to 348 K could be resulted from the segmental movement with the temperatures increase. However, the increase in the electrical conductivity is linear beyond 330 K as observed for other systems [32-33].
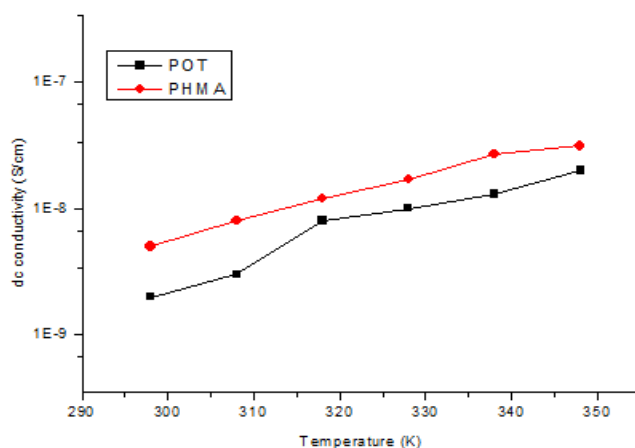

Figure 17: DC conductivity for POT and PHMA with different temperatures
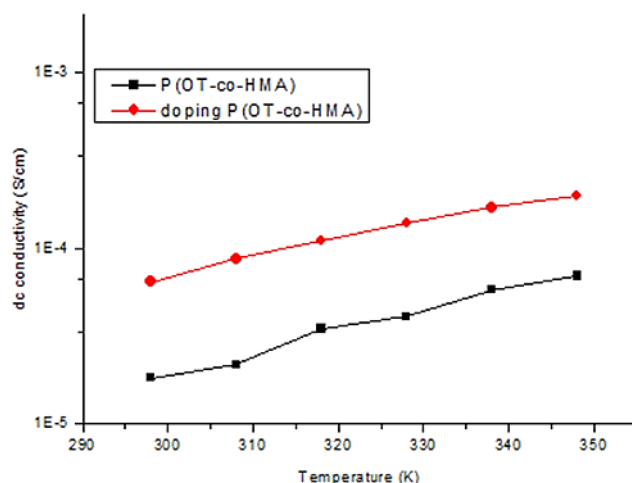
Figure 18: DC conductivity for P(OT-co-HMA) and doping P(OT-co-HMA) with different temperatures

Conclusions

Conducting composite polymers was successfully synthesized. Fourier Transform Infrared and Thermogravimetric analysis was used to confirm the synthesized polymer. The electrical conductivity and activation energy for the polymers was measured by two probe method and found the conductivity increase in the order of doping P(OT-co-HMA)> P(OT-co-HMA)> PHMA >POT. When there is an increase in the temperature, there is an increase in the conductivity, which is similar to the behavior of the semiconducting materials.

Acknowledgments

I would like to extend my deep appreciation and sincere thanks to Professor Anis A.Al Najar. The same goes to technical staff at the department of chemistry for providing the necessary technical assistance and support in the experimental.

Funding

This research did not receive any specific grant from fundig agencies in the public, commercial, or not-for-profit sectors.

Authors' contributions

All authors contributed toward data analysis, drafting and revising the paper and agreed to responsible for all the aspects of this work.

Conflict of Interest

We have no conflicts of interest to disclose.

ORCID:

Samah Hussein Kadhim

https://www.orcid.org/0000-0001-8782-1028

References

[1]. Nezakati T., Seifalian A., Tan A., Seifalian A.M., *Chem. Rev.*, 2018, **118**:6766 [Crossref], [Google scholar], [Publisher]

[2]. Nguyen D.N., Yoon H., *Polymers*, 2016, **8**:118 [Crossref], [Google scholar], [Publisher]

[3]. Kausar A., *J. Macromol. Sci.*, 2017, **54**:640 [Crossref], [Google scholar], [Publisher]

[4]. Kim J., Lee J., You J., Park M.S., Hossain M.S.A., Yamauchi Y., Kim J.H., *Mater. Horiz.*, 2016, **3**:517 [Crossref], [Google scholar], [Publisher]

[5]. Kim J., Kim J.H., Ariga K., *Joule*, 2017, **1**:739 [Crossref], [Google scholar], [Publisher]

[6]. Wang Y., Mayorga-Martinez C.C., Pumera M., *Bull. Chem. Soc. Jpn.*, 2017, **90**:847 [Crossref], [Google scholar], [Publisher]

[7]. Li G., Shrotriya V., Huang J., Yao Y., Moriarty T., Emery K., Yang Y., *Mater. Sustain. Energy*, 2011, 80 [Crossref], [Google scholar], [Publisher]

[8]. Lu W., Fadeev A.G., Qi B., Mattes B.R., *J. Electrochem. Soc.*, 2004, **151**:H33 [Crossref], [Google scholar], [Publisher]

[9]. Camurlu P., *RSc Adv.*, 2014, **4**:55832 [Crossref], [Google scholar], [Publisher]

[10]. Pandey R.K., Lakshminarayanan V., *Appl. Catal. B: Environ.*, 2012, **125**:271 [Crossref], [Google scholar], [Publisher]

[11]. Zhou Q., Shi G., *J. Am. Chem. Soc.*, 2016, **138**:2868 [Crossref], [Google scholar], [Publisher]

[12]. Wang G., Morrin A., Li M., Liu N., Luo X., *J. Mater. Chem. B,* 2018, **6**:4173 [Crossref], [Google scholar], [Publisher]

[13]. Lange U., Roznyatovskaya N.V., Mirsky V.M., *Anal. Chim. Acta.*, 2008, **614**:1 [Crossref], [Google scholar], [Publisher]

[14]. Samia M.M., Auhood K., Zainab M. K., *J. Edu. Pure Sci. Uni. Thi-Qar*, 2021, **11**:122

[15]. Teran-Jimenez O., Rodriguez-Roldan G., Hernandez-Rivera D., Suaste-Gomez E., IEEE Sens. J., 2017, **17**:2492 [Crossref], [Google scholar], [Publisher]

[16]. Naveen M.H., Gurudatt N.G., Shim Y.B., *Appl. Mater. Today*, 2017, **9**:419 [Crossref], [Google scholar], [Publisher]

[17]. Park S., Park C., Yoon H., *Polymers*, 2017, **9**:155 [Crossref], [Google scholar], [Publisher]

[18]. Wang Y., Michinobu T., *Bull. Chem. Soc. Jpn.*, 2017, **90**:1388 [Crossref], [Google scholar], [Publisher]

[19]. Ravichandran R., Sundarrajan S., Venugopal J.R., Mukherjee S., Ramakrishna S., *J. R. Soc. Interface*, 2010, **7**:S559 [Crossref], [Google scholar], [Publisher]

[20]. Wang X., Gu X., Yuan C., Chen S., Zhang P., Zhang T., Yao J., Chen F., Chen G., *J. Biomed. Mater. Res.*, 2004, **68A**:411 [Crossref], [Google scholar], [Publisher]

[21]. Humpolicek P., Kasparkova V., Saha P., Stejskal J., *Synth. Met.*, 2012, **162**:722 [Crossref], [Google scholar], [Publisher]

[22]. Tomczykowa M., Plonska-Brzezinska M.E., *Polymers*, 2019, **11**:350 [Crossref], [Google scholar], [Publisher]

[23]. Hu C., Zheng Y., Qing Y., Wang F., Mo C., Mo Q., *J. Wuhan Univ. Technol. Mater. Sci. Ed.*, 2016, **31**:937 [Crossref], [Google scholar], [Publisher]

[24]. Dhanavela S., Nivethaaa E.A.K., Sangamithiraia D., Narayananb V., Stephena A., *Int. J. Innov. Res. Sci. Eng.*, 2018, 1 [Google scholar], [Publisher]

[25]. Kondawar S.B., Hedau M.J., *Mod. Phys. Lett. B*, 2006, **20**:1461 [Crossref], [Google scholar], [Publisher]

[26]. Manglik N., Jain R., Pramod K.S., Bhattacharya B., Vijay S., Tomar S., *High Perform. Polym.*, 2017, **29**:266 [Crossref], [Google scholar], [Publisher]

[27]. Tieli Z., Xiuhong X., Jianyan C., Liying Y., Weidong R., *Polym. Bull.*, 2016, **73**:621 [Crossref], [Google scholar], [Publisher],

[28]. Ramesh K.S., Velmurugan R., Edison D., Sekar M., *Int. J. Trend Res. Dev.*, 2016, **3**:591 Google scholar], [Publisher]

[29]. Safenaz M.R., Sheikha M., *Adv. Mater. Phys. Chem.*, 2012, **2**:75 [Crossref], [Google scholar], [Publisher]

[30]. Umare S.S., Shambharkar B.H., Ningthoujam R.S., *Synth. Met.*, 2010, **160**:1815 [Crossref], [Google scholar], [Publisher]

[31]. Ghosh A., Mondal A., *Appl. Surf. Sci.*, 2015, **328**:63 [Crossref], [Google scholar], [Publisher].

[32]. Islam S., Lakshmi G.B.V.S., Siddiqui A.M., Husain M., Zulfequar M., *Int. J. Polym. Sci.*, 2013, **2013** [Crossref], [Google scholar], [Publisher]

[33]. Murad S. K., Kadhim S. H., Int. J. Pharm. Res., 2020, **12**,2, 264 [Crossref], [Google scholar], [Publisher]